Application of CDM-PI-P Controller for SO_2 Emission Control Process

C. Maheswari*, K. Krishnamurthy*, B. Meenakshipriya*, P.K. Bhaba**

**Department of Mechatronics Engineering, School of Building and Mechanical Sciences, Kongu Engineering College, Perundurai, Tamil Nadu, India.*
E-mail: {maheswarikec, krish9842722881, b.meenakshipriya}@gmail.com
***Department of Chemical Engineering, Annamalai University, Annamalainagar, Tamil Nadu, India. (E-mail: pkbhaba@gmail.com)*

Abstract: This paper focuses on the sulphur dioxide (SO_2) emission control using PI-P controller by considering Coefficient Diagram Method (CDM) as a candidate. To analyse the removal efficiency of SO_2, liquid-gas absorption column with mixing unit is modelled using SIMULINK in MATLAB platform. Sulphuric acid containing hydrogen peroxide is used as a scrubbing liquid. To compute the parameters of the CDM-PI-P controller, process is approximated as First Order Plus Time Delay (FOPTD) transfer function model. Performance of the CDM-PI-P controller is analysed and compared with conventional control techniques such as Ziegler-Nichols PI controller (ZN-PI) and Internal Model Control based PI controller (IMC-PI) in terms of time domain performance measures such as settling time, rise time, overshoot (t_s, t_r, $\%M_p$) and error indices (ISE, IAE, ITAE). The simulation results prove that the CDM-PI-P controller provides most consistent performance as compared to the conventional controllers.

Keywords: CDM-PI-P controller, SO_2 emission control, Liquid-Gas absorption column.

1. INTRODUCTION

One of the most taxing contaminant that must be removed from the industrial flue gas is sulphur dioxide (SO_2). The main sources of SO_2 emissions are coal fired boilers, sulphuric acid plants, chemical and metallurgical furnaces. Many techniques have been proposed for SO_2 removal process such as conversion of SO_2 into sulphur (Zhihui Ban, 2004), wet flue gas desulphurization, dry flue gas desulphurization, semi dry flue gas desulphurization (Yuegui Zhou et al., 2009), activated carbon (Azargohar et al., 2009) etc. Among all the techniques, wet type flue gas desulphurization produces 60-95% removal efficiency (Cofalaa et al., 2004).

Several researchers have tried many absorbents for wet technique to obtain better removal efficiency. Among these, lime stone based flue gas desulphurization technique is most widely used since it gives more than 90% SO_2 removal efficiency. Even though this technique provides better removal efficiency, it produces CO_2 as a secondary emission (Edward et al., 2004; Sheng-yu Liu et al., 2008). Thus, for the desulphurization process, sulphuric acid with added hydrogen peroxide is used as a reactant and it produces sulphuric acid as a by-product without generating any other pollutants (US patent no: 5,595,713). This technique is proved with experimental investigations and hence it is considered for this work.

Based on the results given in (Sandrine Colle et al., 2004), the flow rate and concentration of hydrogen peroxide has the direct influence on outlet SO_2 concentration. For regulating the flow rate of hydrogen peroxide, an appropriate controller is required to improve the removal efficiency by reducing outlet SO_2 concentration. From the literature review, Alpbaz (2006) has developed a self tuning PID controller for lime stone desulphurization process, but so far no controller is developed for H_2O_2 based desulphurization process. Hence a simple and robust controller is needed for this process.

Coefficient Diagram Method (CDM) is a systematic method introduced by Prof. Shunji Manabe in 1991. It is an algebraic approach that combines classical and modern control theories. In CDM, the polynomial matrices are used for plant and controller representation. CDM controller is designed in such a way that it produces a convenient bandwidth and response without an overshoot. CDM is a more complex controller as compared to conventional PID controller, but it provides convenient parameter selection rules to design a controller under the conditions of stability, robustness and time domain performances (Manabe, 1998). Hence a simple and robust controller, CDM based PI-P, is proposed for SO_2 emission control process.

The structure of the paper is as follows: A brief description about SO_2 emission control process and its model development is presented in section 2. The design of controllers such as ZN-PI, IMC-PI and CDM-PI-P controller are covered in section 3. Section 4 emphasizes the simulation results, comparative studies and performance measures. The final section summarizes the major conclusions of the proposed work. Various sources pertaining to this work are listed in the references.

2. PROCESS DYNAMICS AND MODELING

2.1 Process Description

Absorption is the process of transforming a gaseous pollutant from gas phase to a liquid phase. It involves the removal of gaseous pollutants by dissolving them in a liquid (Sinnott, 1991). For this process, packed column is designed based on the principle of gas-liquid interface to obtain proper liquid to gas mixing. It leads to the efficient removal of soluble SO_2 from gas stream. The liquid-gas absorption process using Liquid-Gas absorption column is illustrated in Figure1.

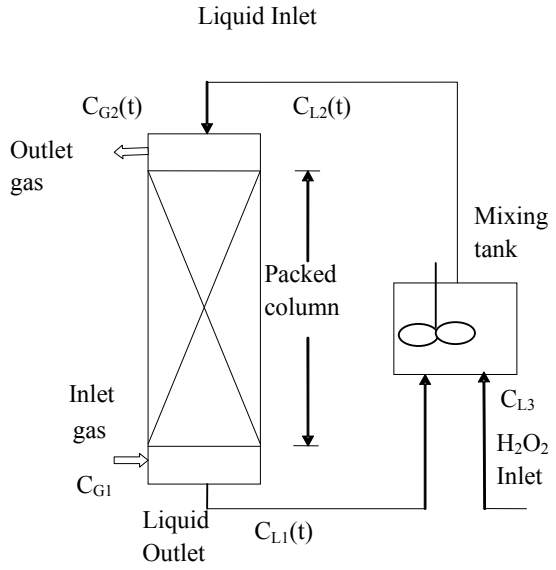

C_{L1} (t)	=	Concentration of H_2O_2+H_2SO_4 exit from the bottom of column (mol/L)
C_{L2} (t)	=	Concentration of H_2O_2+H_2SO_4 entering into the top of column (mol/L)
C_{G2} (t)	=	Concentration of SO_2 in outlet gas stream (mol/L)
C_{L3}	=	Concentration of H_2O_2 entering in to the mixing tank (mol/L)
C_{G1}	=	Concentration of SO_2 in inlet gas stream (mol/L)
G_1	=	Gas flow rate for the column (m^3/hr)
L_1	=	Liquid flow rate for the column (lph)
L_2 (t)	=	Liquid flow rate in to the mixing tank (lph)
V	=	Volume of the mixing tank (L)

Fig. 1. Schematic of SO_2 absorption process.

The SO_2 gas is entered at the inlet stream of the packed column. At the outlet, the mixing tank contains the sulphuric acid with added hydrogen peroxide which is used as a solvent to absorb the inlet SO_2 gas. The stirrer is employed in the mixing tank to mix the solvent homogenously.

The oxidation reaction occurred inside the liquid-gas absorption column which is expressed as:

$$SO_2 + H_2O_2 \longrightarrow H^+ + HSO_4^- \longrightarrow 2H^+ + SO_4^{2-} \quad (1)$$

The resultant liquid contains sulphuric acid with little amount of untreated hydrogen peroxide which is recirculated through mixing the tank until the hydrogen peroxide solution completely reacts with the SO_2 gas. To improve the removal efficiency, the hydrogen peroxide is added in the mixing tank through final control element for the entire process. After treatment, SO_2 gas is exhausted through the outlet stream of the liquid-gas absorption column.

2.2. Process Dynamics

The following assumptions are made for model development,

1. The sulphuric acid with hydrogen peroxide solvent is recycled continuously.
2. The absorption process in the packed column is counter current.
3. The column operates with a constant temperature.
4. The H_2O_2 concentration is depleted on reacting with SO_2 at a certain time, t.
5. Chemical reactions take place only with hydrogen peroxide and SO_2.

The absorption process is described by the following dynamic equation based on the two-film double resistance theory proposed by (Whitman, 1923).

SO_2 lost by gas stream = SO_2 taken up by the liquid stream

$$G_1\left[C_{G1} - C_{G2}(t)\right] = L_1\left[C_{L1}(t) - C_{L2}(t)\right] \quad (2)$$

The concentration of SO_2 in the exhaust gas stream is obtained from the above equation as follows

$$C_{G2}(t) = C_{G1} - \frac{L_1}{G_1}\left[C_{L1}(t) - C_{L2}(t)\right] \quad (3)$$

The above equation is used to represent the dynamics of liquid-gas absorption column. Material balance around the mixing tank is written by

$$V\frac{dC_{L2}(t)}{dt} = C_{L3}L_2(t) + L_1\left[C_{L1}(t) - C_{L2}(t)\right] \quad (4)$$

The mass balance (4) is obtained by applying the conservation principle on the mixing tank with inlet concentrations (C_{L1} (t), C_{L3}) and outlet concentration C_{L2} (t).

The rate equation is expressed for the mass transfer and chemical reaction between gas and liquid. It is represented as a first order differential equation since the complete conversion is not obtained without recirculation (Octave levenspiel, 2004). By considering the reaction rate of SO_2 on H_2O_2, the general rate equation (5) is formulated as,

$$-r_A = \frac{dC_A}{dt} = K_2C_AC_B \quad (5)$$

Where, r_A – reaction rate, C_A – concentration of component A, C_B – concentration of component B, K_2 - reaction rate constant. The above equation is rewritten for the liquid-gas absorption column is given by:

$$\frac{dC_{L1}(t)}{dt} = K_2C_{G1}C_{L2}(t) \quad (6)$$

The rate of change of outlet liquid concentration C_{L1} (t) depends both on the inlet SO_2 concentration (C_{G1}) as well as the inlet liquid concentration (C_{L2} (t)).

2.3. Model development

Based on the dynamics of mixing tank (4) and liquid-gas absorption column (2) and (6) as shown in Figure 2, the SIMULINK model of SO_2 emission control system in MATLB platform is developed.

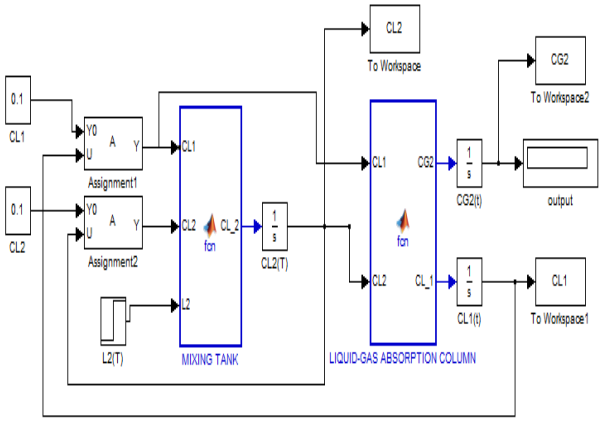

Fig. 2. MATLAB-SIMULINK model of SO_2 emission control process.

The model parameters are tabulated in Table 1. The flow rate of hydrogen peroxide is varied from (0 - 1) lph with a sampling interval of 0.01 lph and the corresponding steady state outlet SO_2 concentrations are measured.

The typical pattern of a steady state process reaction curve as shown in Figure 3 is obtained by plotting the measured steady state outlet SO_2 concentrations (mol/L) (controlled variable) against flow rate of hydrogen peroxide (lph) (manipulated variable). This reaction curve is normally used to describe the characteristics of SO_2 emission control process. From Figure 3, it is clear that the behaviour of the process is nonlinear and stable. Hence, First Order Plus Time Delay (FOPTD) transfer function $(G(s) = \frac{K_P}{\tau_P s + 1} e^{-\theta s})$ model is used to represent the SO_2 emission control process.

Table 1. Parameters for SO_2 emission control process.

Sl. No.	Parameter	Values
1.	Liquid flow rate for the column (L_1)	150 lph
2.	Gas flow rate for the column (G_1)	40 m^3/h
3.	Concentration of H_2O_2 entering in to the mixing tank (C_{L3})	0.1 mol/L
4.	Liquid flow rate in to the mixing tank (L_2(t))	0-1 lph
5.	Initial concentration of Concentration of H_2O_2+H_2SO_4 exit from the bottom of columnC_{L1}(t)	0.1 mol/L
6.	Concentration of H_2O_2+H_2SO_4 entering into the top of column C_{L2}(t)	0.1 mol/L
7.	Concentration of SO_2 in inlet gas stream (C_{G1})	0.12 mol/L

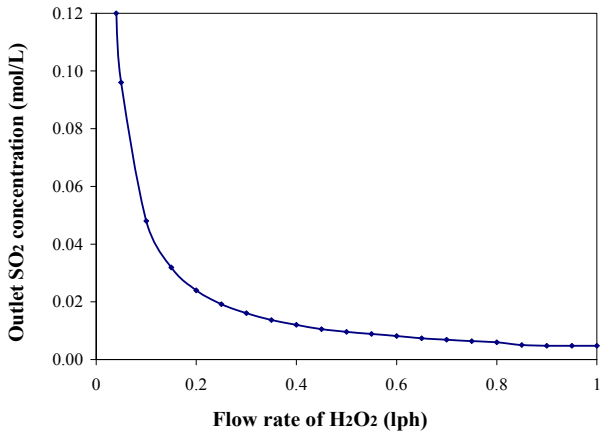

Fig. 3. Steady state process reaction curve of SO_2 emission control system.

For model identification, the simulation runs are carried out at different nominal operating points of outlet SO_2 concentrations 0.048mol/L, 0.016mol/L and 0.0048mol/L. In the open loop scheme, the operating point of 0.0048mol/L is maintained by regulating the flow rate of hydrogen peroxide. Then, a step change with a magnitude of ±10% is given to the flow rate of hydrogen peroxide. As a consequence, the value of outlet SO_2 concentration varies and this variation is recorded against time until a new steady state is attained. The recorded data are plotted against time to get the reaction curve by which the first order model parameters (process gain K_p and process time constant τ_p) of SO_2 emission control process are determined (Gopal, 2002). The same procedure is repeated for other operating points of 0.016 mol/L and 0.048 mol/L outlet SO_2 concentrations. The identified model parameters are tabulated in Table 2.

Table 2. Identified model parameters at different operating points of outlet SO_2 concentrations.

Operating point		Step Magnitude	K_p (%/%)	τ_p (Sec)
Outlet SO_2 Concentration (mol/L)	SO_2 removal efficiency (%)			
0.048	60	10%	14.56	251
		-10%	**27**	249
0.016	86.67	10%	26.96	250
		-10%	2.56	245
0.0048	96.67	10%	0.44	**244**
		-10%	2.407	254

From Table 2, it is clear that the large gain variations are obtained at different magnitudes and it shows that the system is non-linear. The worst case model with the largest process

gain (K_p=27) and smallest time constant (τ_P=244) is selected to represent the SO_2 emission control process. The identified FOPTD model of the process is represented as,

$$G(s) = \frac{K_P}{\tau_P s + 1} e^{-\theta s} = \frac{27}{244S + 1} e^{-s} \quad (7)$$

Where, the process delay (θ) is considered as 1 sec which is the sampling time used for simulation runs.

3. CONTROLLER DESIGN

3.1. Conventional PI controllers

Many previous researchers have used the performance of a conventional PI controller as the benchmark to analyse the performance of a proposed controller. In this way, the conventional PI controllers such as Ziegler-Nichols PI controller (Ziegler and Nichols, 1942) and Internal Model Control based PI controller (Sigurd Skogestad, 2001) are considered for comparative purpose. For convenience, these control techniques are abbreviated as ZN-PI and IMC-PI respectively. The settings of the above said controllers are computed based on the FOPTD model given in (7) and are provided in Table 3.

Table 3. Conventional PI Controller Parameters.

Controllers	Tuning Rules	Parameters		
		K_c	T_i (sec)	$K_i = (K_c/T_i)$
ZN-PI (Ziegler and Nichols 1942)	$K_c = \frac{0.9\tau_P}{\theta K_P}$ and $T_i = 3.33\theta$	8.133	3.33	2.442
IMC-PI (Sigurd Skogestad 2001)	$K_c = \frac{\tau_P + 0.5\theta}{K_P(\lambda)}$ and $T_i = \tau_p + 0.5\theta$	5.326	244.5	0.0217
where, K_c - Controller gain; K_p - Process gain; K_i - Integral gain; τ_p - Process time constant; T_i - Integral time constant; θ - Process delay; λ - Tuning factor (Recommended value 1.7θ)				

3.2 CDM-PI-P controller

The CDM-PI-P controller parameters are computed based on design procedure given in (Meenakshipriya et al., 2011). The general form of two-degrees of freedom (2DOF) PI control structure is shown in Figure 4.

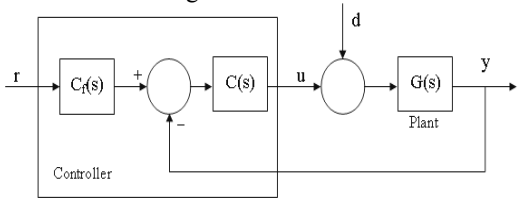

Fig. 4. Two-degree of freedom PI control structure.

$$C(s) = \frac{B(s)}{A(s)} = \frac{k_1 s + k_0}{s} \quad (8)$$

$$C_f(s) = \frac{F(s)}{B(s)} = \frac{k_0}{k_1 s + k_0} \quad (9)$$

Where, A(s) - forward denominator polynomial; B(s) - feedback numerator polynomial; F(s) - reference numerator polynomial; k_0 and k_1 – Coefficients of CDM controller polynomials. By using the CDM controller polynomials of A(s) and B(s) from (8), the characteristic polynomial P(s) is obtained as follows.

$$P(s) = A(s)D(s) + B(s)N(s) = \sum_{i=0}^{n} a_i s^i, a_i > 0 \quad (10)$$

Where, N(s) and D(s) are the numerator and denominator polynomials of the plant transfer function.

The target characteristics polynomial ($P_{target}(s)$) is determined as

$$P_{target}(s) = a_0 \left[\left\{ \sum_{i=2}^{n} \left(\prod_{j=1}^{i-1} \frac{1}{\gamma^j} \binom{i-1}{i-j} \right) (\tau s)^i \right\} + \tau s + 1 \right] \quad (11)$$

Where τ - Equivalent time constant ($\tau = t_s / 2.5 \approx 3$) and γ_i - Stability indices ([2.5 2 2 …]). By equating the polynomials (10) and (11), the values of the CDM controller polynomials (k_1 and k_0) and equivalent time constant (τ) are computed as follows.

The process considered for this study is approximated as FOPTD transfer function model. Hence the general mathematical model is given below.

$$G_P(s) = \frac{N(s)}{D(s)} = \frac{K_P}{\tau_P s + 1} e^{-\theta s} \quad (12)$$

Using a simple first order Pade approximation for dead time in the Laplace domain, $e^{-\theta s} = \frac{2 - \theta s}{2 + \theta s}$, (12) becomes

$$G_P(s) = \frac{N(s)}{D(s)} = \frac{2K_P - K_P\theta s}{\tau_P \theta s^2 + (2\tau_P + \theta)s + 2} \quad (13)$$

By substituting (8) and (13) in (10), the characteristic polynomial of the control system is obtained as

$$P(s) = (s)(\tau_P \theta s^2 + (2\tau_P + \theta)s + 2) + (k_1 s + k_0)(2K_P - K_P\theta s)$$
$$= \tau_P \theta s^3 + (2\tau_P + \theta - k_1 K_P \theta)s^2 + (2 + 2k_1 K_P - K_P k_0 \theta)s + 2K_P k_0 \quad (14)$$

By substituting the value of equivalent time constant (τ) and the stability indices $\gamma_i = \{\gamma_1, \gamma_2\}$ in (11), the target characteristic polynomial is formulated as

$$P_{target}(s) = a_0 \left[\frac{\tau^3}{\gamma_2 \gamma_1^2} s^3 + \frac{\tau^2}{\gamma_1} s^2 + \tau s + 1 \right] \quad (15)$$

The stability indices (γ_1 and γ_2) are selected based on Manabe's recommended value or the designer can change the value of stability indices, if required. However, the equivalent time constant (τ) is not specified and it is considered as another variable to be solved.

By equating the coefficients of the terms of equal power of (14) and (15), equivalent time constant (τ) and CDM controller parameters (k_1 and k_0) are computed as follows.

$$\tau = \left(\frac{\tau_P \theta \gamma_1^2 \gamma_2}{a_0}\right)^{1/3}, \quad k_1 = \left(\frac{a_0 \tau + K_P k_0 \theta - 2}{a_0}\right), \quad k_0 = \left(\frac{a_0}{2K_P}\right) \tag{16}$$

By using the above equation, CDM-PI-P controller parameters (K_c, T_i and K_f) in terms of CDM controller polynomials (k_1 and k_0) are obtained as follows.

The block diagram (Figure 5) shows the general PI-P control structure where G(s), $G_{PI}(s)$ and $G_P(s)$ represent the transfer function models of the plant, PI controller ($G_{PI}(s) = K_c\left(1 + \frac{1}{T_i s}\right)$) and P controller ($G_P(s) = K_f$) respectively. The PI-P control system given in Figure 5 is reduced to its equivalent system as shown in Figure 6.

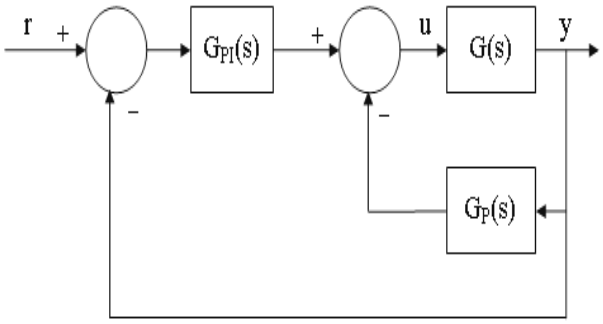

Fig. 5. Block diagram of PI–P control system.

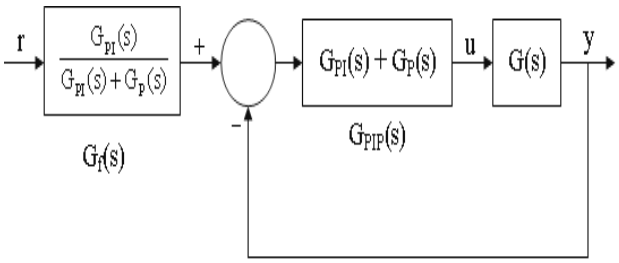

Fig. 6. Equivalent PI-P control system.

From Figure 6, it is observed that $G_{PIP}(s)$ and $G_f(s)$ becomes,

$$G_{PIP}(s) = G_{PI}(s) + \frac{(K_c + K_f)T_i s + K_c}{T_i s} \tag{17}$$

$$G_f(s) = \frac{G_{PI}(s)}{G_{PI}(s) + G_P(s)} = \frac{(K_c(1 + T_i s)}{(K_c + K_f)T_i s + K_c} \tag{18}$$

By using the relation $K_c = \lambda K_f$ (Astrom and Hagglund, 1984) in (17) and (18), CDM-PI-P controller parameters and pre-filter elements are found to be

$$K_c = \frac{\lambda k_1}{(1+\lambda)} \quad ; \quad T_i = \frac{\lambda k_1}{(1+\lambda)k_0}$$

$$K_f = \frac{k_1}{(1+\lambda)} \quad \text{and} \quad G_f(s) = \frac{(K_c(1 + T_i s)}{(K_c + K_f)T_i s + K_c} \tag{19}$$

3.2.1. Selection of tuning factor (λ) and stability indices (γ_1, γ_2)

The selection of tuning factor (λ) and stability indices (γ_1, γ_2) are playing a predominant role to obtain the optimal controller settings for CDM-PI-P controller. These parameters have the direct influence on transient control of the closed loop response. The effect of stability indices on closed loop response is analysed at the operating point of 0.06 mol/L SO_2 outlet concentration for minimum λ value of 0.1. Initially, for this analysis, the stability indices are chosen based on the Manabe's recommended value as γ_1=2.5 and γ_2 =2. The closed loop responses are recorded as shown in Figure 7 by increasing each stability indices value at the sampling interval of 0.5.

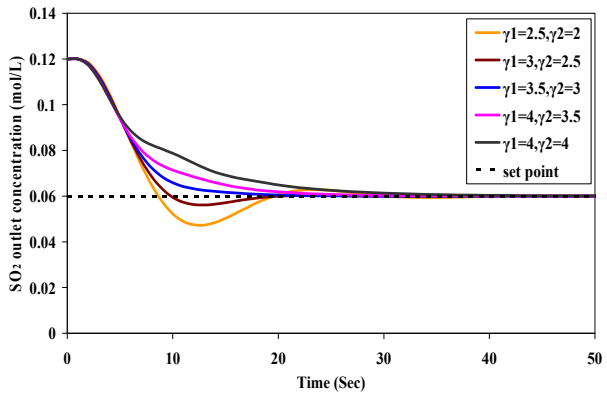

Fig. 7. Effect of stability indices γ_1, γ_2 on the closed loop response for λ=0.1.

From the recorded response, the performance measures are computed and tabulated in Table 4. From the table, it is clear that the performance for γ_1=3.5 and γ_2 =3 is provided fair transient response with minimum settling time and no peak overshoot. Hence γ_1=3.5 and γ_2 =3 are selected as the optimal stability indices values. Similarly, the effect of λ on the closed loop response is studied at the same operating point of 0.06 mol/L SO_2 outlet concentration, by considering the optimized stability indices value of γ_1=3.5 and γ_2=3.

Table 4. Performance measures for the effect of stability indices γ_1, γ_2 on the closed loop response for λ=0.1.

Performance measures	γ_1=2.5, γ_2=2	γ_1=3, γ_2=2.5	γ_1=3.5, γ_2=3	γ_1=4, γ_2=3.5	γ_1=4, γ_2=4
ISE	0.015	0.014	0.015	0.015	0.017
IAE	0.40	0.33	0.33	0.39	0.49
ITAE	2.74	1.39	1.46	2.27	3.92
t_r(Sec)	9	10	NIL	NIL	NIL
t_s(Sec)	128	51	47	102	126
%M_p	21	6.33	NIL	NIL	NIL

The closed loop responses are shown in Figure 8 and the performance measures are computed and tabulated in Table 5.

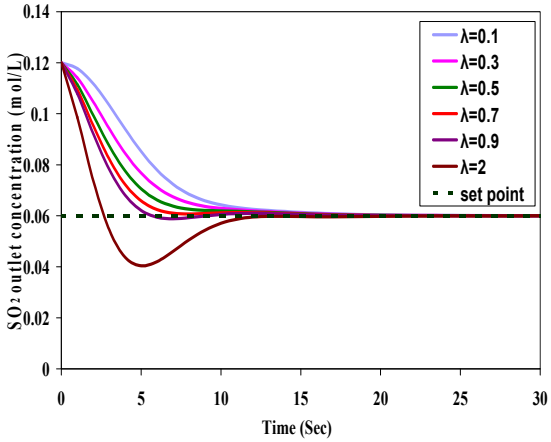

Fig. 8. Effect of tuning factor λ on the closed loop response for γ_1=3.5 and γ_2 =3.

Table 5. Performance measures for the effect of tuning factor λ on the closed loop response for γ1=3.5 and γ2 =3.

Performance Measures	λ=0.1	λ=0.3	λ=0.5	λ=0.7	λ=0.9	λ=2
ISE	0.014	0.010	0.009	0.007	0.007	0.008
IAE	0.34	0.28	0.23	0.19	0.20	0.21
ITAE	1.128	0.812	0.571	0.402	0.491	0.684
t_r (Sec)	NIL	NIL	NIL	NIL	NIL	4
t_s(Sec)	44	43	42	39	42	42
%Mp	NIL	NIL	NIL	NIL	NIL	33

From Figure 8 and Table 5, it is observed that, at λ=0.7, the closed loop response with minimum error indices and less settling time is obtained when compared to other λ values. Hence λ =0.7 is selected as the optimized value for further analysis.

3.2.2. Computation of CDM-PI-P controller parameters

The CDM-PI-P controller parameters are computed based on the procedure given in the section 3.2 as follows.

STEP 1: FOPTD Model of SO_2 emission control system represented in (7) is

$$G(s) = \frac{K_P}{\tau_P s + 1} e^{-\theta s} = \frac{27}{244s + 1} e^{-s}$$

STEP 2: Equivalent transfer function of the above said FOPTD model using first order Pade's approximation technique is

$$G(s) = \frac{-27s + 54}{244s^2 + 489s + 2}$$

STEP 3: First degree CDM controller polynomials (A(s) and B(s)) are chosen as $A(s) = s$ and $B(s) = k_1 s + k_0$

STEP 4: Selected stability indices values (γ_1, γ_2) and tuning factor (λ) are

$\gamma_1 = 3.5$, $\gamma_2 = 3$ and $\lambda = 0.7$

STEP 5: Calculated $P(s) = s\,(244s^2+489s+2) + (k_1 s+k_0)\,(-27s +54)$

STEP 6: Computed coefficients of CDM controller polynomials are k_1= 3.8778 and k_0= 0.54

STEP 7: Comparing the CDM controller polynomials with PI-P controller transfer function, the CDM-PI-P controller parameters (K_c, T_i and K_f) and pre-filter element ($G_f(s)$) are computed as follows:

4. SIMULATION RESULTS

The simulation runs are carried out to analyse the performance of the CDM-PI-P controller with the existing conventional PI control techniques such as ZN-PI and IMC-PI. For analysis, PI controller structure for SO_2 emission control system is modelled using MATLAB-SIMULINK as shown in Figures 9 and 10.From the figures, it can be seen that it is the unity feedback controller which makes the system less sensitive to external disturbances.

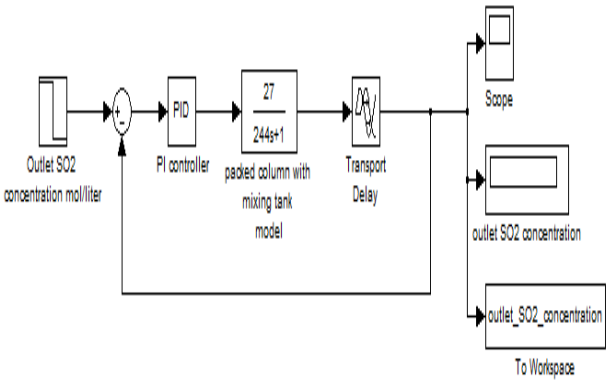

Fig. 9. Model of SO_2 emission control system with conventional PI controller.

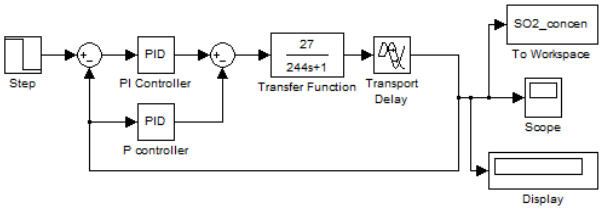

Fig.10. Model of SO_2 emission control system with CDM-PI-P controller

4.1. Performance Analysis

The performance along with controller output of ZN-PI, IMC-PI and CDM-PI-P controllers are analyzed at the operating point of 0.06 mol/L outlet SO_2 concentration and it is recorded in Figures 11 and 12.

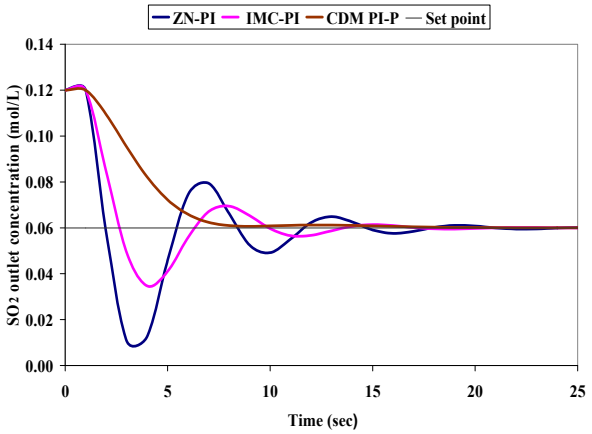

Fig. 11. Performance of CDM-PI-P, ZN-PI and IMC-PI controllers at the operating point of 0.06 mol/L SO_2 outlet concentration.

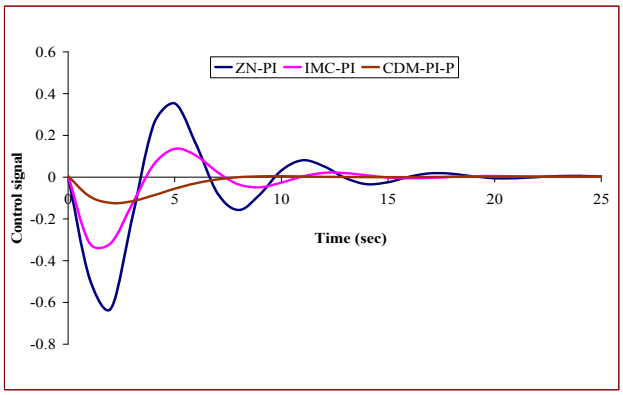

Fig. 12. Effect of control signals on CDM-PI-P, ZN-PI and IMC-PI controllers .

From the figures, it is clear that the CDM-PI-P controller is forced to follow the set point at short duration of time and maintain the steady state without overshoot as compared to ZN-PI and IMC-PI control techniques.

Similarly, the same analysis are carried out with different operating points such as 0.09 mol/L (25% removal efficiency), 0.06 mol/L (50% removal efficiency), 0.03 mol/L (75% removal efficiency), 0.02 mol/L (83.4% removal efficiency), 0.01 mol/L (92% removal efficiency) to ensure the robustness of the CDM-PI-P controller.

Closed loop simulated transient responses obtained at different operating points are shown in Figure 13. The figure reveals that the performance of CDM-PI-P provides better performance with the same settings for different operating points. Among the controller tuning rules, CDM-PI-P tolerates the perturbations in the model parameters and provides the most consistent and robust response when the operating point changes.

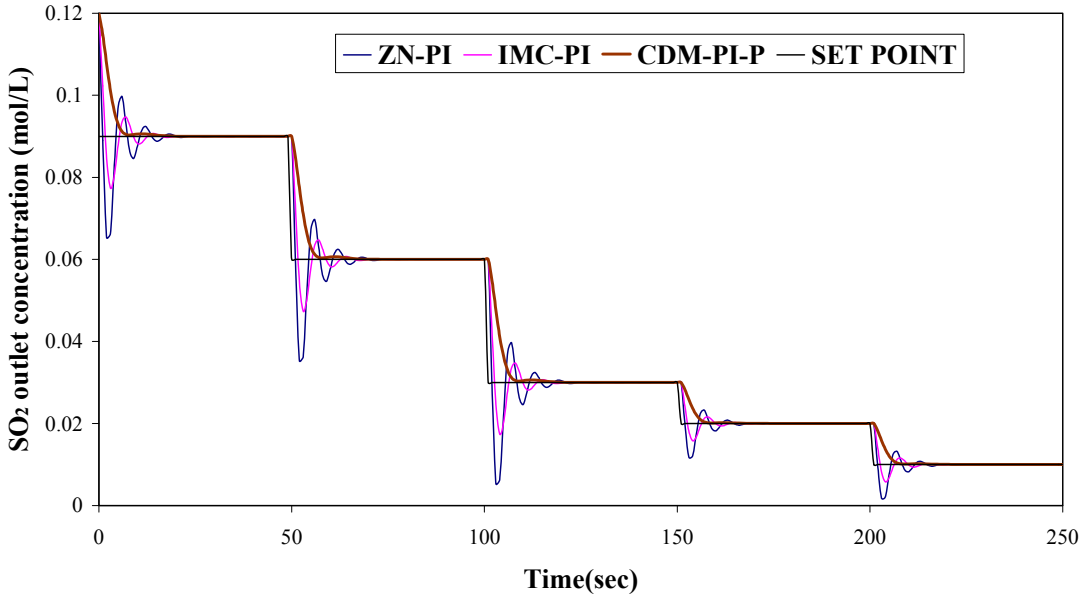

Fig.13. Servo responses for different set point tracking.

Table 6. Performance measures of the controllers at different operating points.

Operating points (mol/L)	Removal Efficiency (%)	Performance measures	ZN-PI	IMC-PI	CDM-PI-P
0.09	25	ISE	0.0003	0.0004	0.001
		IAE	0.04	0.0405	0.03
		ITAE	0.1	0.07	0.04
		t_r (Sec)	4	5	NIL
		t_s (Sec)	50	350	40
		%Mp	27.7	22.2	NIL
0.06	50	ISE	0.0003	0.0004	0.001
		IAE	0.04	0.04	0.03
		ITAE	0.1	0.07	0.04
		t_r (Sec)	4	5	NIL
		t_s (Sec)	50	220	40
		%Mp	46.6	16.6	NIL
0.03	75	ISE	0.0003	0.0004	0.001
		IAE	0.04	0.04	0.03
		ITAE	0.1	0.04	0.03
		t_r (Sec)	4	5	NIL
		t_s (Sec)	50	255	40
		%Mp	20.3	10	NIL
0.02	83.4	ISE	0.0003	0.00004	0.0001
		IAE	0.014	0.013	0.012
		ITAE	0.035	0.024	0.014
		t_r (Sec)	15	10	NIL
		t_s (Sec)	55	340	35
		%Mp	41.5	25	NIL
0.01	92	ISE	0.0003	0.00004	0.0001
		IAE	0.014	0.013	0.012
		ITAE	0.035	0.023	0.014
		t_r (Sec)	15	10	NIL
		t_s (Sec)	55	56	35
		%Mp	90	50	NIL

The performance measures in terms of error indices such as Integral Squared Error (ISE), Integral Absolute Error (IAE), Integral Time Absolute Error (ITAE)), and Quality indices such as (rise time t_r, settling time t_s, peak overshoot $\%M_p$) derived from Figure 13 are tabulated in Table 6. The numerical values presented in Table 6 reveal that the minimum error indices and good quality indices are obtained by the CDM-PI-P controller.

From the simulation results, it becomes clear that the CDM-PI-P controller is effective for controlling the nonlinear process. Though there are variations in the process gain, better control action is achieved by bringing the system to the desired set value without any modifications in the controller design and structure. The developed SO_2-H_2O_2 absorption model provides fair simulation results over different range of operating points.

4.2 Disturbance rejection test

The disturbance rejection performance is investigated at the operating point of 0.06 mol/L outlet SO_2 concentration. A step disturbance is introduced into the process by way of increasing the outlet SO_2 concentration to 0.09 mol/L after 30^{th} second as shown in Figure 14.

From the figure, it is ensured that, only CDM-PI-P controller damp the disturbance in a shorter time with no undershoot as compared to the ZN-PI and IMC-PI controllers. The error and quality indices of output signal are used to evaluate the disturbance rejection performance of the controllers and are given in Table 7.

Table 7. Performance measures after disturbance at the operating point of 0.06 mol/L outlet SO_2 concentrations.

Performance Measures	ZN-PI	IMC-PI	CDM-PI-P
ISE	0.011	0.016	0.011
IAE	0.594	0.666	0.480
ITAE	10.93	8.92	8.42
t_r (Sec)	8	9	-
t_s (Sec)	83	98	44
%Mp	46.16	25.57	NIL

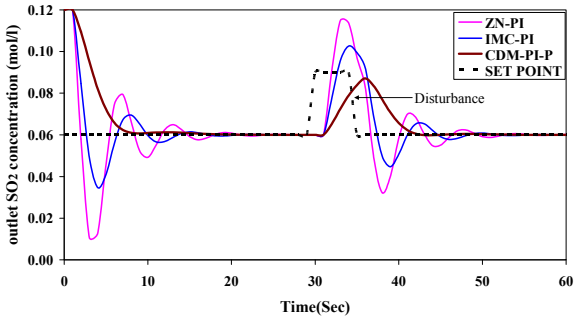

Fig.14. Closed loop response with disturbance at the operating point of 0.06 mol/L outlet SO_2 concentration

From the results, it is proved that the CDM-PI-P control strategy is also successful in disturbance rejection with minimum error indices and good quality indices.

5. CONCLUSIONS

In this work, SO_2 emission control was achieved through the CDM-PI-P controller. SO_2 emission control process was developed based on the Liquid-Gas absorption kinetics principle in SIMULINK at MATLAB platform. The developed SO_2-H_2O_2 absorption model provides fair simulation results over different range of operating points. From the process, it was observed that the outlet SO_2 concentration depends on the flow rate of hydrogen peroxide. Since hydrogen peroxide is a stringent component, it boosts up the oxidation process during the absorption of SO_2. Thus perfect control over the flow the rate of hydrogen peroxide was made by the CDM-PI-P controller. From the simulation results, it was proved that the CDM-PI-P controller provides fair transient as well as steady state behaviour with minimum error indices and good quality indices than the ZN-PI and IMC-PI controllers. Among the controller tuning rules, CDM-PI-P controller tolerated the perturbations in the model parameters when the operating point changes. Also, it produces successful performance in disturbance rejection test. Finally it is concluded that CDM furnishes a convenient and flexible design under the conditions of stability, robustness, and time domain performance which provides superior performance in terms of set point tracking and disturbance rejection.

GREEK SYMBOLS

τ : Equivalent time constant
τ_p : Process time constant
θ : Process delay
γ_i : Stability indices

ABBREVIATIONS

CDM	:	Coefficient Diagram Method
CDM-PI-P	:	Coefficient Diagram Method-Proportional Integral-Proportional
FOPTD	:	First Order Plus Time Delay
ISE	:	Integral Squared Error
IAE	:	Integral Absolute Error
IMC-PI	:	Internal Model Control-Proportional Integral
PI	:	Proportional Integral
ZN-PI	:	Ziegler Nichols-Proportional Integral

NOMENCLATURE

A(s)	:	Forward denominator polynomial of the controller transfer function
B(s)	:	Feedback numerator polynomial of the controller transfer function
C_A	:	Concentration of component A(mol/L)
C_B	:	Concentration of component B(mol/L)
$CL_1(t)$	:	Concentration of H_2O_2+H_2SO_4 exit from the bottom of column (mol/L)
$CL_2(t)$	:	Concentration of H_2O_2+H_2SO_4 entering into the top of column (mol/L)
CL_3	:	Concentration of H_2O_2 entering in to the mixing tank (mol/L)
C_{G1}	:	Concentration of SO_2 inlet to the Gas-Liquid absorption column (mol/L)
C(s)	:	Main controller
$C_f(s)$	:	Feed forward controller
F(s)	:	Reference numerator polynomial of the controller transfer function
G1	:	Gas flow rate for the column (m^3/hr)
H_2O_2	:	Hydrogen peroxide
H_2SO_4	:	Sulphuric acid
l_i, k_i and a_i	:	Coefficients of CDM controller polynomials
L1	:	Liquid inlet flow rate for the column (lph)
$L_2(t)$	:	Liquid Flow rate in to the mixing tank (lph)
%Mp	:	Percentage peak overshoot
N(s)	:	Numerator polynomial of the plant transfer function
P(s)	:	Characteristic polynomial of the closed-loop system
$P_{target}(s)$	:	Target characteristic polynomial of the closed-loop system
r_A	:	Reaction rate
SO_2	:	Sulphur dioxide
t_r	:	Rise time
t_s	:	Settling time
V	:	Volume of the tank (L)

REFERENCES

Alpbaz, M., Hapog lu, H., Ozkan, G., and Altuntas, S. (2006). Application of self-tuning PID control to a reactor of limestone slurry titrated with sulfuric acid. *Chemical Engineering Journal*, 116, 19–24.

Astrom, K. J., and Hagglund, T. (1984). Automatic tuning of simple regulators with specifications on phase and amplitude margins. *Automatica*, 20, 645-651.

Azargohar, R., and Dalai, A.K. (2006). Reduction of sulphur gas emissions using activated carbon. *In proceedings of the IEEE conference proceedings on EIC Climate Change Technology,* 1-10. Ottawa, ON.

Cofalaa, Amanna, J.M., Gyarfasa, F., Schoeppa, W., Boudrib, J.C., and Hordijka. L. (2004). Cost-effective control of SO_2 emissions in Asia. *Journal of Environmental Management*, 72, 149-161.

Edward, S., Rubin, Sonia Yeh, and David, A. Hounshell. (2004). Experience curves for power plant emission control technologies. *Energy technology and policy*, 2, 52-70.

Gopal, M. (2002). *Control Systems: Principles and Design*, Tata McGraw-Hill, New Delhi.

Hydrogen peroxide for Flue Gas Desulphurization. US patent no: 5,595,713.

Manabe, S. (1998). Coefficient diagram method. *In Proceedings of the 14th IFAC Symposium on Automatic Control in Aerospace*, August 24-28, Seoul, Korea, 199-210.

Meenakshipriya, B., Saravanan, K., Somasundaram, S., and Bhaba, P.K. (2011).CDM-based PI-P control strategy in pH neutralization system, *Instrumentation Science & Technology*.39(3), 273 – 287.

Octave levenpiel. (2004). *Chemical Reaction Engineering*. Wiley, Newyork.

Sandrine Colle, Jacques Vanderschuren, and Diane Thomas. (2004). Pilot-scale validation of the kinetics of SO_2 absorption into sulfuric acid solutions containing hydrogen peroxide. *Chemical Engineering and Processing*, 43,1397-1402.

Sheng-yu Liu, Pei Liu, Jin Gao, Jian-ying Liu, Zhi-xiang Ye, and Cheng-hua Xu. (2008). Simulation studies on limestone dissolution with organic acid additives in limestone based flue gas desulfurization. *In proceedings of International conference on bioinformatics and Biomedical Engineering*, *IEEE explore*.3899 – 3902.

Sigrud Skogestad (2001). Probably the best simple PID tuning rules in the world. *AIChE Annual Meeting*, Reno, Nevada.

Sinnott, R.K. (1991). *Coulson & Richardson's chemical engineering design*, Jordan Hill, Oxford, ISBN: 0750665386.

Whitman,W.G.(1923).*Chemical and metallurgical Engineering*, 29-147.

Yuegui Zhou, Xian Zhu, Jun Peng, Yaobin Liu, Dingwang Zhang, and Mingchuan Zhang. (2009). The effect of hydrogen peroxide solution on so_2 removal in the semidry flue gas desulphurization process. *Journal of Hazardous Materials*, 170,436–442.

Zhihui Ban, Jinchang Zhang, Shudong Wang, and Diyong Wu. (2004). Direct Reduction of SO_2 to elemental sulfur by the coupling of cold plasma and catalyst(I), *Industrial and Engineering Chemistry Research*,43,5000-5005.

Ziegler, J.G., and Nichols, N.B., (1942). Optimum settings for automatic controllers. *Transaction of the A.S.M.E.,* 64,759–768.